Comparing three different *Phaeodactylum tricornutum* strains for the production of chrysolaminarin in flat panel airlift photobioreactors

Konstantin Frick[1,2] · Yen-Cheng Yeh[2] · Ulrike Schmid-Staiger[2] · Günter E. M. Tovar[1,2]

Abstract

In recent years, various applications for algae-based ß-1,3-glucans have been postulated, including animal feed and human nutrition. Chrysolaminarin is a ß-1,3–1,6-glucan produced by diatoms such as *Phaeodactylum tricornutum* for energy storage. It is accumulated under nutrient-depleted cultivation conditions. In this study, the production of chrysolaminarin in artificially illuminated scalable flat panel airlift photobioreactors (FPA) was investigated by using *P. tricornutum* in a two-stage production process. In the growth stage primarily biomass is produced, and the subsequent nitrogen-depleted stage induces the accumulation of chrysolaminarin. Three *P. tricornutum* strains (SAG 1090-1a, SAG 1090-1b, SAG 1090–6) were cultured at laboratory scale in 6 L-FPA reactors under controlled light conditions to characterize the process and identify a production strain. The chrysolaminarin content of the algae strains was analysed and additionally their contents of eicosapentaenoic acid and fucoxanthin, both of which could be involved in a possible co-production. Strain SAG 1090-1b exhibited the highest biomass productivity and chrysolaminarin content (317 ± 9 mg g_{DW}^{-1}) after nitrogen depletion, and thus stood out as the most suitable for chrysolaminarin production in a two-stage process. A co-production of the three compounds is possible. However, during nitrogen depletion there occurred trade-offs between the compounds. As chrysolaminarin was produced, the amount of fucoxanthin in the culture stagnated or even decreased depending on the selected strain.

Keywords ß-glucan production · Artificial illumination · *Phaeodactylum tricornutum* · Chrysolaminarin · Fucoxanthin · Eicosapentaenoic acid

Introduction

Microalgae are considered to play an important role in many future technologies and concepts, from bioeconomy to space travel (Nagarajan et al. 2020; Revellame et al. 2021). Microalgae produce different interesting compounds such as fatty acids which can be used for biofuels (Lam and Lee 2012) as well as high value compounds like β-carotene or astaxanthin (Vonshak 1990). In diatoms, targeted valuable products are mainly fucoxanthin (FX) and eicosapentaenoic acid (EPA) (Derwenskus

et al. 2020a; Yang et al. 2020). Recently, the ß-glucan chrysolaminarin (CRY) has gained considerable attention due to its attractive potential applications (Caballero et al. 2016; Reis et al. 2021; Gora et al. 2022).

Chrysolaminaran is a water soluble (1,3)-(1,6)-ß-D-glucan which serves as an energy and carbon storage in diatoms and is especially accumulated during nutrient depletion (Myklestad 1989; Størseth et al. 2006; Kroth et al. 2008; Xia et al. 2014; Gao et al. 2017). Various effects of CRY have already been described in humans and animals. CRY derived from the diatom *Synedra acus* shows antitumor activity (Kusaikin et al. 2010). Recently it could be shown that CRY from *Phaeodactylum tricornutum* promotes the health of juvenile fish (Reis et al. 2021). CRY also shows promising results for managing hypercholesterolemia tested in zebra fish as a model organism. The results are comparable to simvastatin, a drug used for controlling cholesterol levels as well as for ß-1,3-glucan derived from yeast (Gora et al. 2022). Therefore, CRY could potentially be used in human

✉ Konstantin Frick
konstantin.frick@igvp.uni-stuttgart.de

1 Institute of Interfacial Process Engineering and Plasma Technology (IGVP), University of Stuttgart, Pfaffenwaldring 31, 70569 Stuttgart, Germany

2 Fraunhofer Institute for Interfacial Engineering and Biotechnology IGB, Nobelstraße 12, 70569 Stuttgart, Germany

nutrition as well. Due to its good solubility in water it could be processed in beverages. Except for a missing mannitol ending and a higher number of 1,6-branches, CRY closely resembles laminarin, a ß-1,3-glucan which can be found in macroalgae (Beattie et al. 1961). The application of laminarin derived from macroalgae already has been examined. It can be used in animal feed due to its immunomodulatory effects or it can be used in agriculture as it triggers defence mechanisms in vascular plants by contact with their leaves (Cardinale et al. 2000; Klarzynski et al. 2000; Aziz et al. 2003; Kogan and Kocher 2007; Stuyven et al. 2009; Ryan et al. 2012; Sweeney et al. 2012). Water-insoluble ß-glucans from different sources, like cereal or yeast are already part of the human diet (Ciecierska et al. 2019) or used for animal feed, in aquaculture (MacroGard™, Offra).

Fucoxanthin (FX) is of interest due to its bioactivity in humans and animals. It is a xanthophyll, which can be found in marine and freshwater micro- and macroalgae and serves as an intracellular light harvesting pigment in diatoms as well as in haptophytes. (Peng et al. 2011). Its anti-oxidative (Sachindra et al. 2007; Heo et al. 2012; Fung et al. 2013), anti-inflammatory (Neumann et al. 2018b), weight-reducing (Maeda et al. 2005, 2006; Gille et al. 2019) and anti-cancer (Kotake-Nara et al. 2001; Hosokawa et al. 2004) properties makes it a promising candidate for an application as a functional ingredient in the food industry as an antioxidative ingredient addressing obesity or in the pharma industry. A first product against non-alcoholic fatty liver disease are already on the market in the United States (Fucovital™, Algatech).

Eicosapntaenoic acd (EPA; 20:5 ω-3) is an omega-3-fatty acid, and found in marine macro- and microalgae (Radwan 1991). It plays an important role in animal and human metabolism (Tassoni et al. 2008). The (sufficient) consumption of EPA is linked to health promoting effects, for example the prevention of cardiovascular diseases (Rambjør et al. 1996; Lee et al. 2009; Oscarsson and Hurt-Camejo 2017). Nevertheless is a low level of omega-3-fatty acids in the blood a widespread problem, especially in regions with a western style diet (Stark et al. 2016) and EPA (for example from fish oil) used as food supplement (Ritter et al. 2013). EPA derived from microalgae has shown a good bioavailability in tests with mice and humans (Neumann et al. 2018a; Stiefvatter et al. 2021).

Flat panel airlift photobioreactors (FPA) are highly efficient photobioreactor systems, which allow high cell concentrations and biomass productivities of up to $1.53 \mathrm{~g~L}^{-1} \mathrm{~day}^{-1}$ have been reported (Derwenskus et al. 2020b). FPA photobioreactors are energy-efficient, commercially available and already used in industrial settings. However, with a volume of up to 180 L, scale-up is necessary for broader application in industry, which is currently done via interconnecting the reactors to a reactor volume of over $5 \mathrm{~m}^3$ (Subitec GmbH 2022). Due to technical progress in recent years, especially

in the field of LEDs, artificial illumination is becoming a viable option to outdoor cultivation with sunlight. First production scenarios are already published (Derwenskus et al. 2020b). Taking into account general ecological aspects as well as possible locations for photobio-productions, artificial illumination or outdoor cultivation may of course be preferred in a given environment.

In their review addressing the production of high value compounds using diatoms, Yang et al. (2020) reported that only a few studies focused on the production of CRY. The only study to date on the production of CRY with *P. tricornutum* in photobioreactors, focused on the influence of the initial nitrogen content in the culture medium without determining the actual beginning of nitrogen depletion (Gao et al. 2017). Moreover, Gao et al. (2017) aimed mainly to obtain lipids in addition to the mentioned compounds and observed a relatively low maximal CRY content of $171 \mathrm{~mg~g}^{-1}$ under the cultivation conditions they applied. Therefore, the aim of this study was to examine the production of CRY with *P. tricornutum* in industrially relevant photobioreactors. This was done by comparing three different *P. tricornutum* strains in order to find a suitable strain for further investigation for CRY production. To address modern biorefinery concepts as well (Derwenskus et al. 2020b), a possible co-production of FX and EPA, which should be possible with *P. tricornutum*, ought to be investigated in addition to an effective production of CRY and for economic reasons.

Materials and methods

Algae strains

Phaeodactylum tricornutum strains SAG 1090-1a (UTEX 642), SAG 1090-1b (UTEX 640) and SAG 1090–6 (UTEX 646) were used. All strains were from the Department of Experimental Phycology and Culture Collection of Algae (EPSAG) of the Georg-August University in Göttingen, Germany. SAG 1090-1b is listed as a marine strain, whereas SAG 1090-1a and SAG 1090–6 are listed as brackish strains (The Culture Collection of Algae at the University of Göttingen 2022a, b, c).

Culture medium

All three *P. tricornutum* strains were cultivated in brackish conditions in modified Mann & Myers medium with $10 \mathrm{~g~L}^{-1}$ NaCl, $2.4 \mathrm{~g~L}^{-1}$ MgSO$_4$ .7H$_2$O, $0.6 \mathrm{~g~L}^{-1}$ CaCl$_2$.2H$_2$O and $20 \mathrm{~mL}^{-1}$ trace element solution. The composition of the trace element solution remained as in the original recipe (Mann and Myers 1968). Phosphate was supplied via a stock solution ($50 \mathrm{~g~L}^{-1}$) made from potassium phosphate. Phosphate content in the reactor was kept

between 20 and 200 mg L^{-1} (0.2—2.1 mmol L^{-1}). Nitrogen was supplied via a stock solution (35 g L^{-1} ammonium) made from ammonium hydrogen carbonate. In the pre-cultures and during the growing stage ammonium content in the reactor was kept between 30 and 300 mg L^{-1} (1.7—16.6 mmol L^{-1}). Ammonium was preferred over nitrate as N-source, as it led to a higher biomass productivity in preliminary trials. During nitrogen depletion, the addition of ammonium was stopped. Ammonium as well as phosphate content was analysed via flow injection analysis.

Experimental setup and reactor control

To examine nutrient repleted (growth) stage, each strain was cultivated in three consecutive fed-batch cultivations for five days (see Fig. 1). The cultures were initially inoculated from

a pre-culture (see Pre-cultures). After five days, the culture was diluted to a biomass concentration of 1 g_{DW} L^{-1} and the next fed-batch was started. The biomass concentration was measured daily (see Determination of biomass concentration) and the light adjusted accordingly (see Light conditions). Biomass samples for analysis were taken at the end of the last fed-batch run. Ammonium and phosphate were added to ensure nutrient repleted conditions.

To examine nitrogen depletion, three batch cultivations were performed (see Fig. 2). For that three separate 6L FPA reactors were inoculated with a biomass concentration of 1 g_{DW} L^{-1} from the same preculture (see Pre-cultures). During the nitrogen depletion stage, the addition of ammonium was stopped and ammonium concentration subsequently dropped to 0 mg L^{-1}. The first day with zero ammonium in the culture medium was set as day 0 of the nitrogen depletion

Fig. 1 Experimental setup to examine the three tested *P. tricornutum* strains under nutrient repleted conditions. For each strain three consecutive runs were made (fed-batch). The starting biomass concentration for each run was 1 g L^{-1}. Each run lasted for 5 days. Afterwards the culture was diluted and the next run started. Light intensity was adjusted daily, nutrients were also replenished daily (see Culture medium)
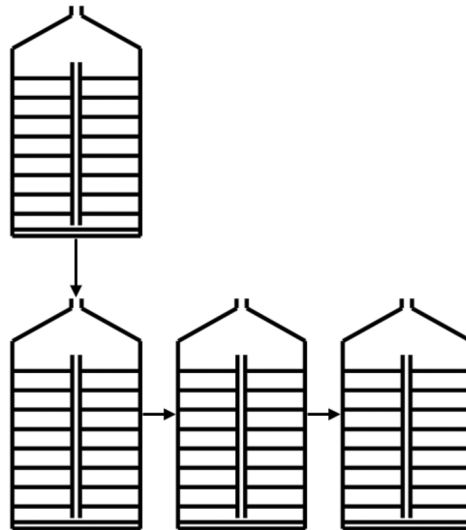
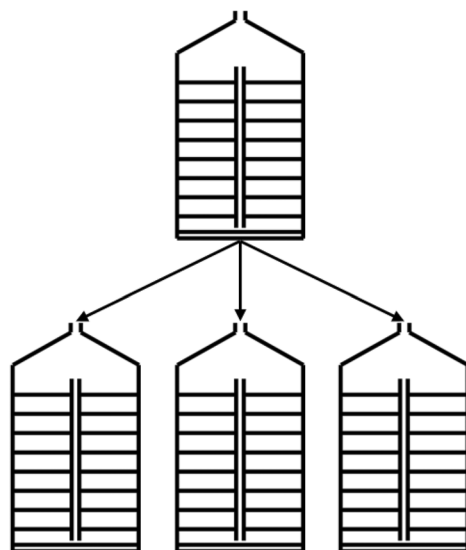Pre-culture
- Biomass concentration measured daily and light adjusted accordingly
- Nutrient repleted cultivation until 3 g_{DW} L^{-1}, afterwards diluted to 1 g_{DW} L^{-1}.
- Cultivation over 14 days prior to experiments

Nitrogen repleted (fed-batch) cultures
- Inoculation at 1 g_{DW} L^{-1}
- Biomass concentration measured daily and light adjusted accordingly
- Nutrient repleted cultivation for 5 days afterwards diluted to 1 g_{DW} L^{-1} for next run
- Overall three consecutive runs

Fig. 2 Experimental setup to examine the three tested *P. tricornutum* strains under nitrogen depleted conditions. Three separate FPA reactors were inoculated with a biomass concentration of 1 g L^{-1} from the same pre-culture. Nitrogen depletion cultivation lasted for 9 days. Light intensity was adjusted daily. The addition of phosphate was continued and the addition of ammonium stopped (see Culture medium).

Pre-culture
- Biomass concentration measured daily and light adjusted accordingly
- Nutrient repleted cultivation until 3 g_{DW} L^{-1}, afterwards diluted to 1 g_{DW} L^{-1}.
- Cultivation over 14 days prior to experiments

Nitrogen depleted cultures
- Inoculation of three separate FPA-reactors at 1 g_{DW} L^{-1} from the same pre-culture
- Biomass concentration measured daily and light adjusted accordingly
- Ammonium addition stopped
- Nutrient depleted cultivation for 9 days
- Daily analysis of CRY, fatty acid (including EPA) and FX content

stage. This was usually the day right after inoculation. During nitrogen depletion stage, dry weight was determined daily and light intensity was adjusted to the new biomass concentration (see Light conditions). In addition, a biomass sample was taken daily for analysis. The experiments ended after 9 days of nitrogen depletion.

All experiments were carried out in flat panel airlift photobioreactors (FPA) with a volume of 6 L (Subitec GmbH, Germany). The FPA reactor is a flat plate reactor with a special design improving the intermixing of the culture and increasing the retention time of the gas bubbles in the culture medium. The FPA is pneumatically mixed by injecting an air/CO_2 mixture through a silicone membrane at the bottom of the reactor.

The setup of the FPA and its peripheral equipment were similar to previous publications (Derwenskus 2020). The pH value was set to 7.3 and varied between 7.1 and 7.5. The air flow was 3 L min^{-1} (0.5 v v^{-1} min^{-1}). The control unit added pure carbon dioxide (1—20 L h^{-1}, 0.5–10% of gas flow) to the air flow automatically in order to keep the pH value of the culture stable. The temperature of the culture varied between 20.0 and 20.5 °C and was regulated via a tempered water bath in which the lower 10 cm of the reactor were immersed. For artificial illumination, the reactors were equipped with LED panels (Nichia, NSSL157AT-H3), placed at one side of the reactor with a distance of 2 cm, illuminating a reactor surface of 0.21 m^2. The light spectrum of the used LEDs was similar to sunlight (3000 K and CRI > 90). The microalgae cultures were illuminated continuously for 24 h. All experiments were carried out at a specific light availability of 5 μmol$_{photons}$ g$_{DW}$$^{-1}$ s^{-1} (see Light conditions for calculations). In previous experiments, this amount of light proved be sufficient to ensure stable growth of *P. tricornutum* in FPA photobioreactors, as well as to minimize stress through high light intensities (Derwenskus et al. 2020a). Cultivation conditions (temperature, addition of CO_2 to air flow, pH, light intensity, addition of ammonium and phosphate) were monitored and controlled via a control unit (Siemens SPS, Germany).

Pre-cultures

Pre-cultures were cultivated under the same conditions as in the experiments. The pre-cultures were cultivated under these conditions for at least 14 days prior to the experiments to minimize adaptation processes during the experiments. By dilution, the biomass concentration was kept between 1 and 3 g$_{DW}$ L^{-1}.

Light conditions

The biomass specific light availability was used to describe the light conditions (Holdmann et al. 2018). The biomass specific light availability correlates the light intensity (photon flux density PFD) on the reactor surface to the volume and the biomass concentration in the microalgae culture. Only light in the PAR region was considered in the calculation. The specific light availability (I_{spec}, dimension: μmol$_{photons}$ g$_{DW}$$^{-1}$ s^{-1}) was calculated according to Eq. 1, with A = illuminated reactor surface (0.21 m^2), PFD = photon flux density on the surface of the reactor (in μmol$_{photons}$ m^{-2} s^{-1}), V = culture volume (6 L), c_{DW} = biomass concentration (in g L^{-1}).

$$I_{spec} = \frac{A * PFD}{V * c_{DW}} \tag{1}$$

All experiments for this publication (nutrient repleted and nitrogen depleted) were conducted with a I_{spec} of 5 μmol$_{photons}$ g$_{DW}$$^{-1}$ s^{-1}. For this purpose, the light intensity was adjusted daily according to the biomass concentration in the culture. During the experiments with nutrient repleted conditions the photon flux density on the reactor surface increased from 140 to up to 720 μmol$_{photons}$ m^{-2} s^{-1} at the end of a fed-batch run. During the experiments concerning nitrogen depleted conditions the light intensity on the reactor surface increased from 140 to up to 360 μmol$_{photons}$ m^{-2} s^{-1}.

Determination of biomass concentration

To determine the biomass concentration, a pre-dried and weighed glass-fibre filter (pore size:0.2 μm; MN 85/70, Macherey–Nagel GmbH, Germany) was placed in a Büchner funnel connected to a small vacuum pump (MZ 2C NT, Vacuubrand GmbH, Germany). A sample (5 mL) was put on the filter. The excess culture medium was removed using the vacuum pump. To remove the remaining culture medium, 5 mL of ddH$_2$O was added to the filter and removed using the pump. This washing step was carried out twice. The filter was then dried (MA 35, Sartorius AG, Germany) and afterwards weighed on an analytical balance (Enteris2241-1S, Sartorius Lab Instruments GmbH, Germany). The biomass concentration was calculated by subtracting the weight of the empty (dry) filter from the weight of the biomass-loaded filter (dry).

Chrysolaminarin analysis

The ß-1,3-glucan content was analysed using an enzymatic test kit (Megazyme, Ireland), which was already previously used for the quantification of (chryso-)laminarin from algae (Danielson et al. 2010). The enzymatic test is based on the enzymatic digestion (β-1,3- glucanase) of CRY and subsequent reaction of the soluble glucose with a glucose oxidase/per-oxidase reagent. The resulting colour shift can be measured photometrically

(McCleary and Draga 2016). The test was conducted according to the manufacturer's instructions, but it was scaled down by the factor of 5. CRY was analysed daily during nitrogen depleted cultivation (biological triplicates, see Fig. 2) as well as at the end of the last run examining nutrient repleted conditions (technical triplicates, see Experimental setup and reactor control).

Fatty acid analysis

The biomass specific fatty acid content (ω_{TFA} in mg g^{-1}) was analysed by applying the transesterification method described by Lepage and Roy (1984). It was executed as previously described by Meiser et al. (2004) using a gas chromatograph (7890A, Agilent, USA). Fatty acids were analysed daily during nitrogen depleted cultivation (biological triplicates, see Fig. 2) as well as at the end of the last run examining nutrient repleted conditions (technical triplicates, see Experimental setup and reactor control).

Fucoxanthin analysis

Determination of the biomass specific FX content (ω_{FX} in mg g^{-1}) was done via HPLC (1200 Infinity, Agilent, USA) based on the method described in (Gille et al. 2015), as described in (Derwenskus et al. 2019). FX was analysed daily during nitrogen depleted cultivation (biological triplicates, see Fig. 2) as well as at the end of the last run examining nutrient repleted conditions (technical triplicates, see Experimental setup and reactor control).

Calculations

Compound concentration

Compound concentration in the culture c_i (dimension mg L^{-1}) was calculated according to Eq. 2 using the biomass concentration c_{DW} (in g L^{-1}) and compound content ω_i (in mg g^{-1}).

$$c_i = c_{DW} * \omega_i \tag{2}$$

The change of the concentration of a compound (i) per litre culture Δc_i (dimension: mg$_i$ L^{-1}) during nitrogen depletion is the difference of the concentration at day n ($c_i (t_n)$) to the concentration at day 0 ($c_i (d_0)$). It was calculated according to Eq. 3 using the biomass concentration c_{DW} (in g L^{-1}) and the biomass specific compound content ω_i (in mg g^{-1}) for the respective day.

$$\Delta c_i = (c_{DW} (tn) * \omega_i (tn)) - (c_{DW} (d0) * \omega_i (d0)) \tag{3}$$

Volumetric productivity

The calculation of the volumetric biomass productivity Q_{DW} (dimension: mg$_{DW}$ L^{-1} day^{-1}) during nutrient repleted and

nitrogen depleted cultivation, was carried out according to Eq. 4 using biomass concentration (in g L^{-1}) at day n (t_n) and at day x (t_x) within a defined process interval. The start of a regarded process interval was defined as day x (t_x) and the end of the process interval as day n (t_n).

$$Q_{DW} = \frac{c_{DW}(tn) - c_{DW}(tx)}{tn - tx} \tag{4}$$

The volumetric compound productivity Q_i (dimension: mg$_i$ L^{-1} day^{-1}) during nitrogen depleted conditions was carried out according to Eq. 5 using the compound concentration (in mg L^{-1}) at day n (t_n) and at day x (t_x) within a defined process interval.

$$Q_i = \frac{c_i (tn) - c_i(tx)}{tn - tx} \tag{5}$$

The content of the regarded compounds CRY, EPA and FX during nutrient repleted conditions were determined as technical triplicates at the end of the last fed-batch run. The volumetric compound productivity during nutrient repleted conditions Q_i was estimated ($Q_{i,est}$) according to Eq. 6 using the mean value of biomass productivity $Q_{DW,mean}$ (in g L^{-1} day^{-1}) and the mean value of compound content $\omega_{i,mean}$ (in mg g^{-1}).

$$Q_{i,est} = Q_{DW,mean} * \omega_{i,mean} \tag{6}$$

Biomass specific compound productivity

The biomass specific compound productivity q_i (dimension: mg$_i$ g$_{DW}$$^{-1}$ day^{-1}) was regarded in a defined process interval. q_i was calculated from the concentration of a component (in mg L^{-1}) at day n ($c_i (t_n)$) and at day x ($c_i (t_x)$), as well as the biomass concentration (in g L^{-1}) at day x ($c_{DW} (t_x)$). It is calculated according to Eq. 7:

$$q_i = \frac{c_i (tn) - c_i (tx)}{c_{DW}(tx) * (tn - tx)} \tag{7}$$

Statistics

The statistical analysis was conducted with the software Matlab R2022a (MathWorks, USA). We used analysis of variance (ANOVA) to examine the statistical significance of the results. The assumptions for ANOVA were tested using the Jarque–Bera test (normality, Matlab function: "jbtest") and the Bartlett's test (equal variances, Matlabfunction"vartestn"). If the assumptions were not met, we used the Kruskal–Wallis test instead of ANOVA to examine the statistical significance of the results. Kruskal–Wallis test is similar to classic analysis of variance (ANOVA) but with less restrictions to the assumptions. Kruskal–Wallis is recommend as the most conservative

strategy when the assumptions for ANOVA can not be assured (Sullivan et al. 2016). The results of ANOVA is shown using F(df1, df2) and p, where F is the F-value, df1 and df2 are the degrees of freedom and p is the p-value. The results of the Kruskal–Wallis test is shown using χ^2 (df1, df2) and p, where χ^2 is the chi-square, df1 and df2 are the degrees of freedom and p is the p-value.

If ANOVA (or Kruskal–Wallis) showed a significant difference, the Tukey post hoc test was conducted to specify the significance between groups. The results of the Tukey post hoc test with $p \leq 0.05$ are indicated in figures and diagrams using lower case letters. Significant differences (significance level $p \leq 0.05$), analysed via ANOVA (or Kruskal–Wallis) with Turkey post hoc test, are indicated with different letters above the columns (figures) or values (tables). Example: If column 1 is indicated with "ab", column 2 with "a" and column 3 with "b", this means that column 1 is not significantly different from column 2 or from column 3. However, columns 2 and 3 are significantly different in this example, because they are marked with different letters. The detailed results of all statistical tests conducted, are presented in Table S5.

Results

In the examined two stage process, the nutrient repleted growth stage serves for biomass production and the nutrient depleted stage is used for the accumulation of CRY. The difference concerning growth respectively biomass productivity and CRY content under nitrogen depleted conditions were determined between the three indicated *Phaeodactylum* strains.

Growth stage

Under nutrient repleted conditions, biomass concentration (C_{DW}) increased in all three *P. tricornutum* strains (see Fig. 3). The biomass productivity (Q_{DW}) differed between the tested strains (see Fig. 4). Strain SAG 1090-1b provided the highest biomass productivity and SAG 1090–6 showed the lowest biomass productivity under the chosen cultivation conditions.

Biomass specific CRY content (ω_{CRY}) was low (under 50 mg g_{DW}^{-1}) during nutrient repleted conditions in all three tested strains (see Table S1). Strain SAG 1090-1b showed a lower ω_{CRY} (12 ± 1 mg g_{DW}^{-1}) compared to strain SAG 1090-1a (47 ± 9 mg g_{DW}^{-1}) and SAG 1090–6 (34 ± 2 mg g_{DW}^{-1}).

Nitrogen depletion stage

Biomass and chrysolaminarin production

Under nitrogen depleted cultivation conditions biomass concentration (C_{DW}) increased in all three tested strains (see
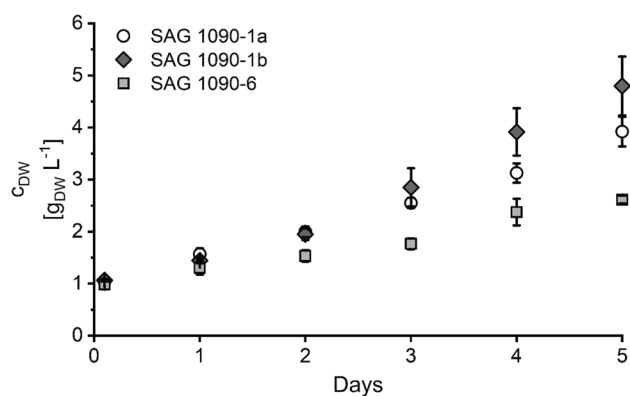

Fig. 3 Biomass concentration c_{DW} of the three tested *P. tricornutum* strains SAG 1090-1a, SAG 1090-1b, and SAG 1090–6 during nitrogen repleted conditions. I_{spec} of 5 $\mu mol_{photons}$ g_{DW}^{-1} s^{-1} was kept constant by daily adaptation of PFD. ($\pm$ SD, n = 3 analysed as biological triplicate
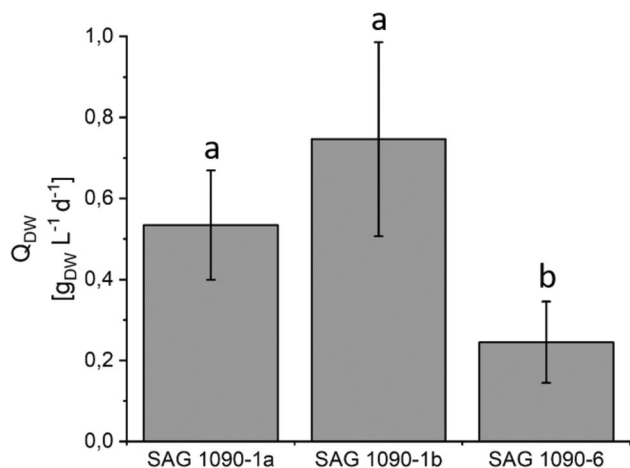

Fig. 4 Biomass productivity Q_{DW} during nutrient repleted conditions of the three tested *P. tricornutum* strains SAG 1090-1a, SAG 1090-1b, and SAG 1090–6. I_{spec} of 5 $\mu mol_{photons}$ g_{DW}^{-1} s^{-1} was kept constant by daily adaptation of PFD. ($\pm$ SD, n = 12 analysed as three groups of biological replicates. Statistics: Different letters above the columns show significant differences (significance level $p \leq 0.05$) analysed via Kruskal–Wallis with Turkey post hoc test. Detailed statistics see Table S5

Fig. 5). The increase in biomass concentration slowed down in the progress of the experiment. Biomass increase stopped with strain SAG 1090–6 and strain SAG 1090-1b after day 4 and with strain SAG 1090-1a after day 7. In the first four days of nitrogen depletion, biomass productivity (Q_{DW}) was stable in all three strains (see Fig. 6). In these first 4 days of nitrogen depletion, Q_{DW} differed between the tested strains. SAG 1090-1b showed the highest and SAG 1090–6 the lowest Q_{DW}. Q_{DW}
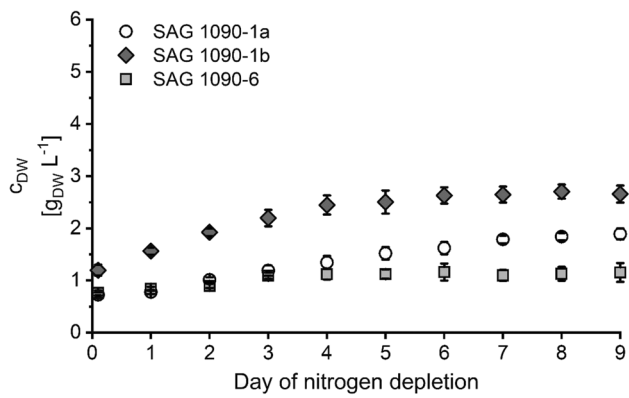
Fig. 5 Biomass concentration of the three tested *P. tricornutum* strains SAG 1090-1a, SAG 1090-1b, and SAG 1090–6 during nitrogen depleted conditions. I_{spec} of 5 $\mu mol_{photons}$ g_{DW}^{-1} s^{-1} was kept constant by daily adaptation of PFD. ($\pm$ SD, n = 3 analysed as biological triplicate
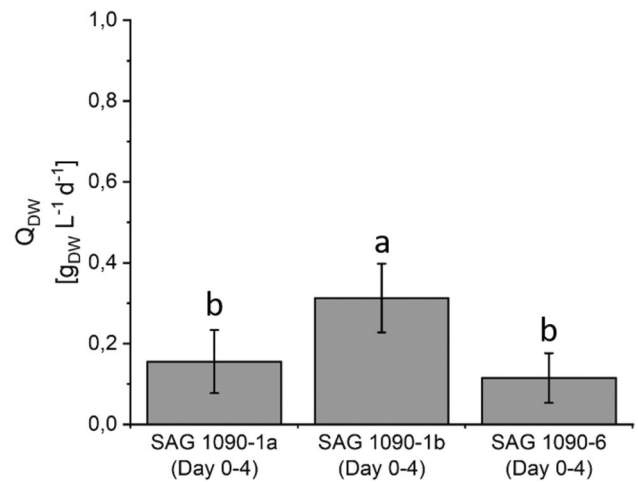

Fig. 6 Biomass productivity Q_{DW} during nitrogen depleted conditions of the three tested *P. tricornutum* strains SAG 1090-1a, SAG 1090-1b, and SAG 1090–6. I_{spec} of 5 $\mu mol_{photons}$ g_{DW}^{-1} s^{-1} was kept constant by daily adaptation of PFD. ($\pm$ SD, n = 12 analysed as three groups of biological replicates. Statistics: Different letters above the columns show significant differences (significance level $p \leq 0.05$) analysed via ANOVA with Turkey post hoc test. Detailed statistics see Table S5

was lower under nitrogen depleted cultivation conditions compared to nitrogen repleted conditions (see Figs. 4 and 6).

After nitrogen depletion the CRY content of the biomass (ω_{CRY}) increased in all three strains. The increase started at day 1 (SAG 1090-1a and SAG 1090-1b) or 2 (SAG 1090–6) of nitrogen depletion. During the progress of the experiment the increase of CRY content ω_{CRY} slowed down in all three strains until remaining constant or even decreasing (see Fig. 7). The maximal CRY content reached, differed between the three strains. Strain SAG 1090-1b showed a higher maximum ω_{CRY} (317 ± 9 mg g_{DW}^{-1}) compared to SAG 1090-1a (210 ± 13 mg g_{DW}^{-1}) and SAG 1090–6 (197 ± 11 mg g_{DW}^{-1}; see Table 1). Even though the highest CRY contents ω_{CRY} were reached at day 7 (SAG 1090-1b) or 9 (SAG 1090-1a and SAG 1090–6) of the nitrogen depletion (see Table 1 and Fig. 7), all three strains reached 90% of their maximum CRY content ω_{CRY} at day 4 (SAG 1090-1b and SAG 1090–6) or day 5 (strain SAG 1090-1a). The highest biomass specific CRY productivity (q_{CRY}) was observed in strain SAG 1090-1b (see Table S4).

Besides ω_{CRY} the content of fatty acids (ω_{TFA}) increased as well during nitrogen depletion in all three tested strains (see Fig. 7). Mainly the content of MUFAs and SFAs increased, whereas the content of PUFAs even decreased, depending on the strain. The increase of ω_{TFA} started subsequent to the accumulation of CRY. Similar to the accumulation of CRY the increase in ω_{TFA} slowed down in the progress of the experiment.

Co-production of chrysolaminarin, fucoxanthin and eicosapentaenoic acid

In contrast to the chrysolaminarin content ω_{CRY}, the fucoxanthin content (ω_{FX}) decreased in all three strains during nitrogen depletion (Table 2). Whereas EPA content (ω_{EPA})

developed differently during nitrogen depletion in the three tested strains. The EPA content ω_{EPA} of strain SAG 1090-1a and strain SAG 1090–6 decreased during nitrogen depletion, whereas the EPA content of SAG 1090-1b increased slightly.

Figure 8 shows the amount of CRY, FX and EPA, which was produced per litre during nitrogen depletion. Even though the general development was similar, there are differences between the three strains. The CRY concentration c_{CRY} increased highest in SAG 1090-1b, but the increase stopped around day 4, whereas in SAG 1090-1a c_{CRY} increased until the end of the experiment. The fucoxanthin concentration c_{FX} decreased fastest in SAG 1090-1b and started to decline immediately after the beginning of nitrogen depletion. Whereas, in SAG 1090-1a and SAG 1090–6 c_{FX} did not decrease in the first days of nitrogen depletion. This can also be seen in the biomass specific FX productivity (see Table S4). Similar to CRY, the highest increase of EPA concentration was observed in SAG 1090-1b.

However, the development of the compound concentrations (c_{CRY}, c_{FX}, c_{EPA}) illustrate the trade-offs between the accumulation of CRY and the production of FX and EPA. Whereas the amount of CRY per litre increased during nitrogen depletion, the amount of FX stagnated (SAG 1090-1a and SAG 1090–6) or even decreased (SAG 1090-1b) during the experiments.

Regarding the EPA production, similar to the biomass increase the EPA concentration increased at the beginning of the nitrogen depletion stage in all three tested strains. However, comparing the estimated volumetric EPA productivity during nitrogen repleted conditions with the volumetric EPA productivity during nitrogen depleted conditions (day 0–4), it showed that

Fig. 7 Chrysolaminarin content ω_{CRY} and fatty acid content ω_{TFA} during nitrogen depletion stage of *P. tricornutum* strain SAG 1090-1a **A** and **D,** SAG 1090-1b **B** and **E**, SAG 1090–6 **C** and **F**. I_{spec} of 5 $\mu mol_{photons}$ g_{DW}^{-1} s^{-1} was kept constant by daily adaptation of PFD. Dotted line marks 90% of the maximum reached ω_{CRY} value of each strain. The fatty acid columns are divided in PUFA (white), MUFA (grey) and SFA (dark grey). ($\pm$ SD, n = 3 analysed as biological triplicates
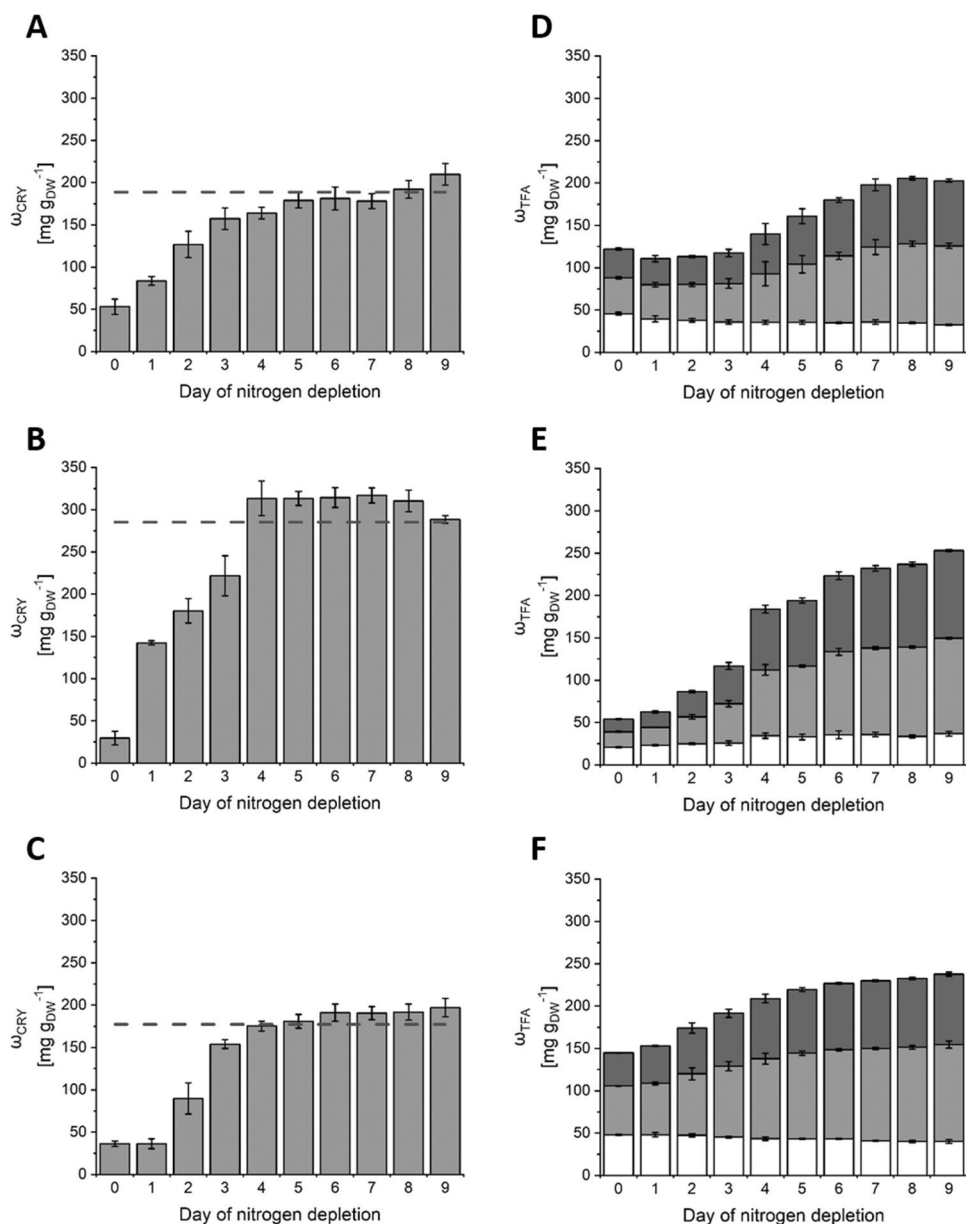
Table 1 Maximum biomass specific chrysolaminarin content ω_{CRY}, of the three tested *P. tricornutum* strains SAG 1090-1a, SAG 1090-1b, and SAG 1090–6 during nitrogen depleted conditions. ($\pm$ SD, n = 3 analysed as biological triplicate). Statistics: Different letters above the values show significant differences (significance level $p \leq 0.05$) analysed via ANOVA with Turkey post hoc test. Detailed statistics see Table S5

		SAG 1090-1a	SAG 1090-1b	SAG 1090–6
Maximum ω_{CRY}	[mg g_{DW}^{-1}]	210 $\pm$ 13 [a] Day 9	317 $\pm$ 9 [b] Day 7	197 $\pm$ 11 [a] Day 9

Table 2 Biomass specific fucoxanthin (FX) content ω_{FX} and eicosapentaenoic acid (EPA) content ω_{EPA} of the three tested *P. tricornutum* strains SAG 1090-1a, SAG 1090-1b, SAG 1090 6 at the beginning of nitrogen depletion (day 0) and at the end of the experiment (Day 9). ($\pm$ SD, n = 3 analysed as biological triplicate)

			SAG 1090-1a	SAG 1090-1b	SAG 1090–6
ω_{FX}	[mg g_{DW}^{-1}]	Day 0	12.0 $\pm$ 0.4	14.4 $\pm$ 0.2	10.2 $\pm$ 0.1
		Day 9	4.0 $\pm$ 0.2	3.5 $\pm$ 0.4	4.2 $\pm$ 0.4
ω_{EPA}	[mg g_{DW}^{-1}]	Day 0	40 $\pm$ 1	20 $\pm$ 1	44 $\pm$ 2
		Day 9	25 $\pm$ 3	23 $\pm$ 1	32 $\pm$ 1
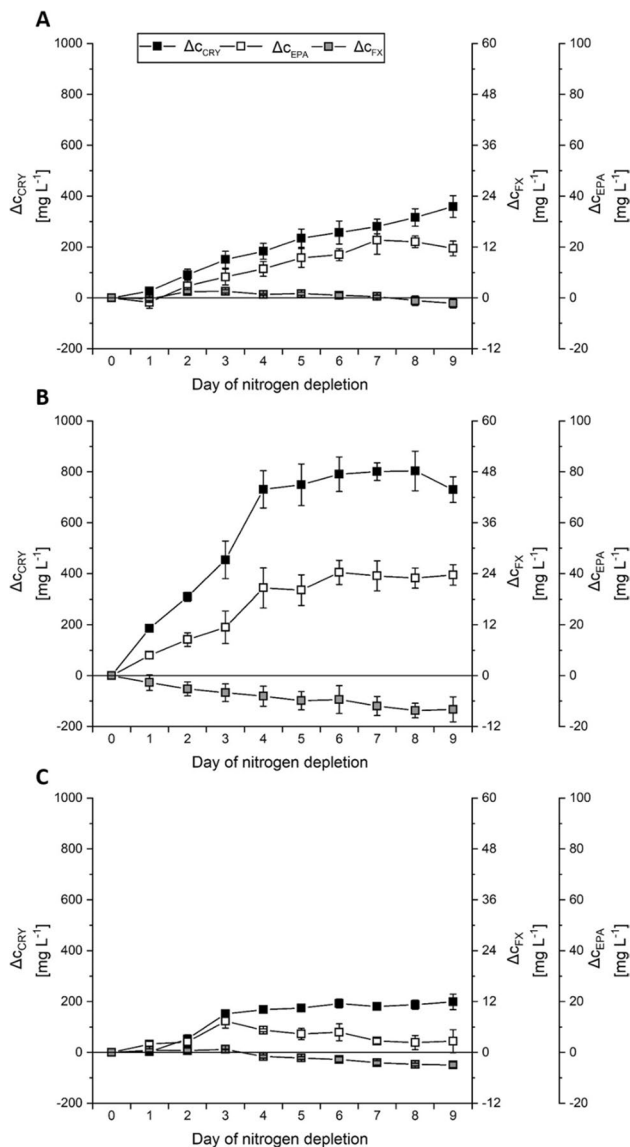
Fig. 8 Change of compound concentration Δc_i (in mg L^{-1}) from CRY (Δc_{CRY}), FX (Δc_{FX}) and EPA (Δc_{EPA}) during nitrogen depletion (compared to day 0) of the three tested strains SAG 1090-1a (A), SAG 1090-1b (B) and SAG 1090–6 (C). Calculation see Compound concentration. I_{spec} of 5 $\mu mol_{photons}$ g_{DW}^{-1} s^{-1} was kept constant by daily adaptation of PFD. ($\pm$ SD, n = 3 analysed as biological triplicate)

volumetric EPA productivity was lower during nitrogen depletion (see Fig. S4).

Discussion

Growth stage

In a two-stage production process of energy storage molecules like CRY, the purpose of the first stage ("growth stage") is to provide biomass. Therefore, a high biomass productivity is beneficial for a production strain. Under the chosen cultivation conditions, strain SAG 1090-1b showed the highest biomass productivity. However, alongside cultivation conditions like light availability, biomass productivity is influenced by the cultivation system. A previous publication reported that in small-scale incubators, strain SAG 1090–6 showed the highest biomass productivity in comparison to strains SAG 1090-1a and SAG 1090-b (Derwenskus et al. 2020a). This difference might be due to the shear forces occurring in FPA reactors, which appear due to their pneumatic operation and structure (Bergmann 2018). Mirón et al. (2003) showed that shear stress caused through aeration in airlift photobioreactors can negatively influence the biomass production of *P. tricornutum*. Overall it is reported that shear forces in photobioreactors can affect the performance of microalgae cultures and put shear stress sensitive algae strains in disadvantage (Mirón et al. 2003; Michels et al. 2016; Wang and Lan 2018). Moreover, *P. tricornutum* shows three different morphotypes (oval, triradiate, and fusiform (Borowitzka and Volcani 1978). The morphotypes might be differently affected by the shear forces in the reactor. Martino et al. (2011) showed that cultivation conditions like temperature and salinity of the culture medium influenced the ratio between the morphotypes. They also showed that this the influence of cultivation conditions on the ratio of the morphotypes differs between *P. tricornutum* strains (Martino et al. 2011). It is possible that the ratio of the morphotypes differed among the tested strains in our experiments and, along with the occurring shear forces, impacted biomass productivity of the strains. Unfortunately the morphotypes were not quantified in our experiments.

CRY is a primary storage carbohydrate and is therefore not accumulated by diatoms under nutrient repleted conditions (Myklestad 1989; Størseth et al. 2006; Kroth et al. 2008; Xia et al. 2014; Gao et al. 2017). In our experiments all tested strains showed a low CRY content ($<$ 50 mg g_{DW}^{-1}) during nitrogen repleted conditions. These results illustrate the need of a second (nitrogen depleted) stage for the accumulation of CRY. Even though low, the CRY content between the three tested strains differed during nitrogen repletion. Unfortunately, the data is not sufficient to conclude, whether the elevated CRY content of SAG 1090-1a indicated a general difference in carbon allocation or if it is a (stress) reaction due to the chosen cultivation conditions (i. e. salinity of the medium, shear forces, specific light availability).

Depletion stage

The depletion stage serves for the production of CRY, a high biomass productivity as well as a fast accumulation of CRY and high CRY content is favourable for a potential

production strain. In our experiments, strain SAG 1090-1b showed the highest biomass productivity. These results align with a previous publication by (Rodolfi et al. 2017), who cultivated *P. tricornutum* SAG 1090-1b and SAG 1090–6 in artificially illuminated 300 mL bubble columns under nitrogen depleted conditions. The highest CRY content was achieved after 7 days of nitrogen depletion using strain SAG 1090-1b (317 ± 9 mg g_{DW}^{-1}). This maximal CRY content is higher compared to Gao et al. (2017), who achieved a maximal CRY content of 171 mg g_{DW}^{-1} while examining the accumulation of CRY in *P. tricornutum* using an artificially illuminated 55-L vertical flat-plate glass photobioreactor.

Even though the highest CRY content was achieved later in depletion stage (see Table 1), our data show that for a future CRY production process in flat panel airlift reactors using *P. tricornutum*, the first four days of nitrogen depletion are crucial. After four (or five) days all three strains already reached 90% of their maximal CRY content and subsequently only a small increase in CRY content was found afterwards. The biomass specific CRY productivity (calculation see Biomass specific compound productivity), was also highest in the first days of nutrient depletion. Further, except for strain SAG 1090-1a, there was only a small increase in CRY concentration after day 4 of nitrogen depletion (see Fig. 8). It is reported, that after a few days of nitrogen depletion, the genes potentially involved in CRY biosynthesis are repressed in diatoms (Kroth et al. 2008; Chauton et al. 2013). Alipanah et al. (2015) examined the response of *P. tricornutum* to nitrogen depletion on a genetic level. They observed the repression of genes related to CRY production after 72 h. This correlates with the results for *P. tricornutum* SAG 1090-1b and SAG 1090–6, where the increase of CRY content, biomass specific CRY productivity, CRY concentration and therefore the production of CRY slowed down strongly after four days of nitrogen depletion (see Figs. 7, 8 and Table S4). However, in strain SAG 1090-1a the biomass specific CRY productivity did not decrease as fast as in the other strains (see Table S4). Moreover, the CRY concentration increased until the end of the observation period (see Fig. 8). This might indicate that strain SAG 1090-1a is regulated differently on a genetic level or that it possesses a larger nitrogen storage that can be mobilized, compared to the other two strains.

Benvenuti et al. (2016) examined a semi-continuous process (with regular nutrient depletion) for the production of fatty acids used for energy storage (TAGs) as an alternative to a batch cultivation using *Nannochloropsis* sp. and achieved promising results. They reported that although TAG content was lower during the semi-continuous process, TAG productivity was similar compared to the batch process, since biomass productivity was higher in the semi-continuous process. Similar to TAGs, CRY is used for energy storage. Based on our results, an approach similar to that of Benvenuti et al. (2016) should be investigated for

the production of CRY and the co-products EPA and FX. The process might consist of a nitrogen repleted stage for biomass production and a short nitrogen depletion stage (2–4 days) for the accumulation of CRY.

As an energy storage molecule, the accumulation of CRY is closely connected to other energy storage compounds, especially fatty acids. Mainly SFAs (C16:0) and MUFAs (C16:1) were produced during nitrogen depletion (see Fig. 7), which is consistent to previous publications (Gao et al. 2017). It is reported, that after a longer stationary phase the carbohydrates are catabolised in favour of the synthesis of fatty acids (Li et al. 2011; Mus et al. 2013; da Costa et al. 2017; Gao et al. 2017). This effect was observed on the last day of nitrogen depletion in SAG 1090-1b. However, the experiments showed that between CRY production and potential CRY catabolism, there is a time window of several days for potential harvesting of CRY-rich biomass.

Some microalgae species accumulate fatty acids as energy storage rather than carbohydrates, whereas other species primarily accumulate carbohydrates as energy storage. The results in our experiments indicate that this is also the case for different strains of the same species. Strain SAG 1090-1b rather accumulated carbohydrates especially in the first days of nutrient depletion, whereas the other two strains accumulated more fatty acids (see Fig. 7).

Co-Production of eicosapentaenoic acid, fucoxanthin and chrysolaminarin

It is possible to produce CRY, FX and EPA in a co-production process (Gao et al. 2017). Unfortunately, it comes to trade-offs between the three compounds as they are produced or accumulated under different cultivation conditions. The FX content and furthermore the FX productivity in microalgae is influenced by the cultivation conditions, especially the light intensity on the reactor surface and biomass specific light availability (Gómez-Loredo et al. 2016; Guo et al. 2016; Derwenskus 2020). The FX contents for the three different strains observed during nutrient repleted conditions in this publication align with previously reported data. For strain SAG 1090-1a cultivated in flasks, Petrushkina et al. (2017) reported a FX content of 10.2 ± 0.6 mg g^{-1}. Guo et al. (2016) reported a FX content of approximately 10 mg g^{-1} for strain SAG 1090–6 grown in flask and Derwenskus et al. (2020a) reported a FX content of 19.1 ± 0.6 mg g^{-1}, for strain SAG 1090-1b grown in illuminated incubators. Furthermore, Nitrogen depletion is not favourable for the production of FX. It is reported that the FX content as well as the content of chlorophyll a and chlorophyll c declined in nitrogen depleted *P. tricornutum* cultures (Huang et al. 2019). Under nitrogen depleted conditions, photosynthesis and chlorophyll associated genes are repressed and no new

pigments are synthesized, not even pigments that do not contain nitrogen such as FX (Alipanah et al. 2015; Derwenskus et al. 2020a). This aligns with our results. During nitrogen depletion, the FX content dropped in all tested strains and the FX concentration in the culture volume did not increase with any strain as well.

Similar to FX, the EPA content decreased as well during nitrogen depletion, except for SAG 1090-1b. In SAG 1090-1b the EPA content even increased slightly in the progress of nitrogen depletion. However, the EPA value of SAG 1090-1b is on a very low level even at the beginning of the depletion, compared to the other two strains and to previously published data by (Alipanah et al. 2015; Derwenskus et al. 2020a). Derwenskus et al. (2020a) reported an EPA content for SAG 1090-1b of 42.8 ± 0.7 mg g_{DW}^{-1} under (nitrogen repleted) growing conditions in FPA reactors. EPA content is influenced by different cultivation conditions such as temperature (Molina et al. 1991), CO_2 concentration or light availability (Molina Grima et al. 1992; Chrismadha and Borowitzka 1994). Although the pre-cultures were cultivated in a similar range of CO_2 concentration, temperature and light availability, the reaction of the strains may have differed. However, a decreasing EPA content during nitrogen depletion aligns with previous publications. It is reported, that the EPA content is constant or decreases during nitrogen depletion (Chrismadha and Borowitzka 1994; Alipanah et al. 2015; Gao et al. 2017). Alipanah et al. (2015) found that the biosynthesis of fatty acids in the chloroplasts is downregulated during nitrogen depletion, which could lead to a stagnating or even declining content of the involved fatty acids, such as EPA. During nutrient repleted conditions, CRY, FX and EPA content were analysed at the end of the last run (see Volumetric productivity). Therefore, the volumetric productivity during nitrogen depleted conditions can only be compared to an estimation of the volumetric productivity during nitrogen repleted conditions (see Figs. S2, S3, S4). Even though the EPA concentration in our experiments increased during nitrogen depletion, the volumetric EPA productivity during nitrogen depleted conditions is lower in all three strains compared to the estimated volumetric productivity during nitrogen repleted conditions, illustrating that nitrogen depletion is not favourable for EPA production. This aligns with previous publications by Molina Grima et al. (1995) who found that EPA productivity in *P. tricornutum* is highest during the nutrient repleted growth phase.

The fact that the three compounds accumulate at different cultivation conditions results in trade-offs. These trade-offs between the three compounds have to be taken into account when designing a co-production process. Depending on the desired biomass composition, the harvesting time and/or the production strain can be varied. Moreover, the influence of other cultivation conditions should also be considered like light availability or CO_2 content. Nunez and Quigg (2016) also showed that the addition of $NaHCO_3$ influenced the fatty acid profile in *P. tricornutum* cultures. For evaluating a co-production process, economic data, like the value of the different components, have to be included as well. Especially the decrease of FX might be an issue, due to its high price. Derwenskus et al. (202b) showed that the value of *P. tricornutum* biomass strongly depends on FX. However, CRY was not included in their study.

Comparison of the tested strains

The results show variations in biomass production and CRY accumulation between the three tested *P. tricornutum* strains. Regarding their suitability for a two-stage production process for the production of CRY, including a nutrient repleted stage for biomass production and a nitrogen depleted stage for CRY accumulation, strain SAG 1090-1b is the most suitable. Strain SAG 1090-1b showed the highest biomass productivity during nutrient repletion (see Fig. 4), as well as the highest CRY content and productivity during nitrogen depleted conditions (see Table 1 and Fig. S2). However, the data are only valid for the chosen cultivation setup. The cultivation system as well as the cultivation conditions have an effect on the economic output of the process considered. For a co-production process, different harvesting scenarios are possible depending on the objective of the process. To illustrate, we developed two potential scenarios based on our results:

Scenario 1 focuses solemnly on the production of CRY. In this scenario a process with a nitrogen depletion phase of four days using strain SAG 1090-1b would be well suited, as this strain showed the highest biomass productivity during nutrient repleted conditions (see Fig. 4) and the highest CRY productivity during nitrogen depleted conditions (see Fig. S2 and Table S4). Furthermore, the increase of CRY concentration and CRY content slowed down after four days of nitrogen depletion (see Figs. 7 and 8).

Scenario 2 focuses on the overall economic output of the process. Here, the amount of FX produced is of great importance for the economy of the process due to its high value (Derwenskus et al. 2020b). In this scenario, a process with a short nitrogen depletion phase (1–2 days) using strain SAG 1090-1b might be well suited. Even though the FX concentration would decrease during nitrogen depletion, the short depletion phase would limit this decrease and the use of strain SAG 1090-1b would ensure that a considerable amount CRY is produced despite the short depletion phase (Fig. 8). It would also be possible to use strain SAG 1090-1a in this scenario, which would be favourable regarding the amount of FX and EPA but unfavourable regarding the amount of CRY produced.

Conclusion

In the artificially illuminated FPA reactors, it was possible to achieve a maximum CRY content ω_{CRY} of 317 ± 9 mg g_{DW}^{-1} under the selected cultivation conditions using *P. tricornutum* strain SAG 1090-1b. To our knowledge, this is the highest CRY content reported for *P. tricornutum* in a photobioreactor. Four days of nitrogen depletion are suitable for the production of CRY, as cultivation under nitrogen depletion for longer than four days led to a decrease in CRY production in favour of the production of fatty acids. For the production of CRY, *P. tricornutum* strain SAG 1090-1b was the best suited from the three tested strains, due to its high biomass productivity in the growth stage and the fast accumulation of CRY in the nitrogen depletion stage.

The results also show that a co-production of all three desired products, CRY, FX, and EPA, is possible using a two-stage process. However. There are trade-offs between the three compounds, as CRY is accumulated during nitrogen depletion, the amount of FX in the culture decreased.

Declarations

References

Alipanah L, Rohloff J, Winge P, Bones AM, Brembu T (2015) Whole-cell response to nitrogen deprivation in the diatom *Phaeodactylum tricornutum*. J Exp Bot 66:6281–6296

Aziz A, Poinssot B, Daire X, Adrian M, Bézier A, Lambert B, Joubert J-M, Pugin A (2003) Laminarin elicits defense responses in grapevine and induces protection against *Botrytis cinerea* and *Plasmopara viticola*. Mol Plant Microbe Interact 16:1118–1128

Beattie A, Hirst EL, Percival E (1961) Studies on the metabolism of the Chrysophyceae. Comparative structural investigations on leucosin (chrysolaminarin) separated from diatoms and laminarin from the brown algae. Biochem J 79:531–537

Benvenuti G, Bosma R, Ji F, Lamers P, Barbosa MJ, Wijffels RH (2016) Batch and semi-continuous microalgal TAG production in lab-scale and outdoor photobioreactors. J Appl Phycol 28:3167–3177

Bergmann P (2018) Operating strategy to reduce the energy consumption of flat-panel airlift photobioreactors with respect to mixing of *Thermosynechococcus elongatus* suspension cultures light-specific adaptation of the superficial gas velocity. Dissertation, University of Hohenheim, Germany.

Borowitzka MA, Volcani BE (1978) The polymorphic diatom *Phaeodactylum tricornutum*: Ultrastructure of its morphotypes. J Phycol 14:10–21

Caballero MA, Jallet D, Shi L, Rithner C, Zhang Y, Peers G (2016) Quantification of chrysolaminarin from the model diatom *Phaeodactylum tricornutum*. Algal Res 20:180–188

Cardinale F, Jonak C, Ligterink W, Niehaus K, Boller T, Hirt H (2000) Differential activation of four specific MAPK pathways by distinct elicitors. J Biol Chem 275:36734–36740

Chauton MS, Olsen Y, Vadstein O (2013) Biomass production from the microalga *Phaeodactylum tricornutum*: Nutrient stress and chemical composition in exponential fed-batch cultures. Biomass Bioenergy 58:87–94

Chrismadha T, Borowitzka MA (1994) Effect of cell density and irradiance on growth, proximate composition and eicosapentaenoic acid production of *Phaeodactylum tricornutum* grown in a tubular photobioreactor. J Appl Phycol 6:67–74

Ciecierska A, Drywień ME, Hamulka J, Sadkowski T (2019) Nutraceutical functions of beta-glucans in human nutrition. Roczniki Państwowego Zakładu Higieny 70:315–324

da Costa F, Le Grand F, Quéré C, Bougaran G, Cadoret JP, Robert R, Soudant P (2017) Effects of growth phase and nitrogen limitation on biochemical composition of two strains of *Tisochrysis lutea*. Algal Res 27:177–189

Danielson ME, Dauth R, Elmasry NA, Langeslay RR, Magee AS, Will PM (2010) Enzymatic method to measure β-1,3-β-1,6-glucan content in extracts and formulated products (GEM assay). J Ag Food Chem 58:10305–10308

Derwenskus F (2020) Entwicklung und Bewertung eines Verfahrens zur Herstellung von Fucoxanthin und Eicosapentaensäure mit *Phaeodactylum tricornutum*. Dissertation, University of Stuttgart, Germany.

Derwenskus F, Metz F, Gille A, Schmid-Staiger U, Briviba K, Schließmann U, Hirth T (2019) Pressurized extraction of unsaturated fatty acids and carotenoids from wet *Chlorella vulgaris* and *Phaeodactylum tricornutum* biomass using subcritical liquids. GCB-Bioenergy 11:335–344

Derwenskus F, Schäfer B, Müller J, Frick K, Gille A, Briviba K, Schmid-Staiger U, Hirth T (2020a) Coproduction of EPA and fucoxanthin with *P. tricornutum* – A promising approach for up- and downstream processing. Chemie Ingenieur Technik 92:1780–1789

Derwenskus F, Weickert S, Lewandowski I, Schmid-Staiger U, Hirth T (2020b) Economic evaluation of up- and downstream scenarios for the co-production of fucoxanthin and eicosapentaenoic acid with *P. tricornutum* using flat-panel airlift photobioreactors with artificial light. Algal Res 51:102078

Fung A, Hamid N, Lu J (2013) Fucoxanthin content and antioxidant properties of *Undaria pinnatifida*. Food Chem 136:1055–1062

Gao B, Chen A, Zhang W, Li A, Zhang C (2017) Co-production of lipids, eicosapentaenoic acid, fucoxanthin, and chrysolaminarin by *Phaeodactylum tricornutum* cultured in a flat-plate photobioreactor under varying nitrogen conditions. J Ocean Univ China 16:916–924

Gille A, Stojnic B, Derwenskus F, Trautmann A, Schmid-Staiger U, Posten C, Briviba K, Palou A, Bonet ML, Ribot J (2019) A lipophilic fucoxanthin-rich *Phaeodactylum tricornutum* extract ameliorates effects of diet-induced obesity in C57BL/6J mice. Nutrients 11:796

Gille A, Trautmann A, Posten C, Briviba K (2015) Bioaccessibility of carotenoids from *Chlorella vulgaris* and *Chlamydomonas reinhardtii*. Int J Food Sci Nutr 67:507–513

Gómez-Loredo A, Benavides J, Rito-Palomares M (2016) Growth kinetics and fucoxanthin production of *Phaeodactylum tricornutum* and *Isochrysis galbana* cultures at different light and agitation conditions. J Appl Phycol 28:849–860

Gora AH, Rehman S, Kiron V, Dias J, Fernandes JMO, Olsvik PA, Siriyappagouder P, Vatsos I, Schmid-Staiger U, Frick K, Cardoso M (2022) Management of hypercholesterolemia through dietary ß-glucans–insights from a zebrafish model. Front Nutr 8:1590

Guo B, Liu B, Yang B, Sun P, Lu X, Liu J, Chen F (2016) Screening of diatom strains and characterization of *Cyclotella cryptica* as a potential fucoxanthin producer. Mar Drugs 14:125

Heo S-J, Yoon W-J, Kim K-N, Oh C, Choi Y-U, Yoon K-T, Kang D-H, Qian Z-J, Choi I-W, Jung W-K (2012) Anti-inflammatory effect of fucoxanthin derivatives isolated from *Sargassum siliquastrum* in lipopolysaccharide-stimulated RAW 264.7 macrophage. Food Chem Toxicol 50:3336–3342

Holdmann C, Schmid-Staiger U, Hornstein H, Hirth T (2018) Keeping the light energy constant — Cultivation of *Chlorella sorokiniana* at different specific light availabilities and different photoperiods. Algal Res 29:61–70

Hosokawa M, Kudo M, Maeda H, Kohno H, Tanaka T, Miyashita K (2004) Fucoxanthin induces apoptosis and enhances the antiproliferative effect of the PPARγ ligand, troglitazone, on colon cancer cells. Biochim Biophys Acta 1675:113–119

Huang B, Marchand J, Blanckaert V, Lukomska E, Ulmann L, Wielgosz-Collin G, Rabesaotra V, Moreau B, Bougaran G, Mimouni V, Morant-Manceau A (2019) Nitrogen and phosphorus limitations induce carbon partitioning and membrane lipid remodelling in the marine diatom *Phaeodactylum tricornutum*. Eur J Phycol 54:342–358

Klarzynski O, Plesse B, Joubert J-M, Yvin J-C, Kopp M, Kloareg B, Fritig B (2000) Linear β-1,3 glucans are elicitors of defense responses in tobacco. Plant Physiol 124:1027–1038

Kogan G, Kocher A (2007) Role of yeast cell wall polysaccharides in pig nutrition and health protection. Livestock Sci 109:161–165

Kotake-Nara E, Kushiro M, Zhang H, Sugawara T, Miyashita K, Nagao A (2001) Carotenoids affect proliferation of human prostate cancer cells. J Nutr 131:3303–3306

Kroth PG, Chiovitti A, Gruber A, Martin-Jezequel V, Mock T, Parker MS, Stanley MS, Kaplan A, Caron L, Weber T, Maheswari U, Armbrust EV, Bowler C (2008) A model for carbohydrate metabolism in the diatom *Phaeodactylum tricornutum* deduced from comparative whole genome analysis. PloS One 3:e1426

Kusaikin MI, Ermakova SP, Shevchenko NM, Isakov VV, Gorshkov AG, Vereshchagin AL, Grachev MA, Zvyagintseva TN (2010) Structural characteristics and antitumor activity of a new chrysolaminaran from the diatom alga *Synedra acus*. Chem Nat Comp 46:1–4

Lam MK, Lee KT (2012) Microalgae biofuels: A critical review of issues, problems and the way forward. Biotechnol Adv 30:673–690

Lee JH, O'Keefe JH, Lavie CJ, Harris WS (2009) Omega-3 fatty acids: Cardiovascular benefits, sources and sustainability. Nat Rev Cardiol 6:753–758

Lepage G, Roy CC (1984) Improved recovery of fatty acid through direct transesterification without prior extraction or purification. J Lipid Res 25:1391–1396

Li Y, Han D, Sommerfeld M, Hu Q (2011) Photosynthetic carbon partitioning and lipid production in the oleaginous microalga *Pseudochlorococcum sp.* (Chlorophyceae) under nitrogen-limited conditions. Bioresour Technol 102:123–129

Maeda H, Hosokawa M, Sashima T, Funayama K, Miyashita K (2005) Fucoxanthin from edible seaweed, *Undaria pinnatifida*, shows antiobesity effect through UCP1 expression in white adipose tissues. Biochim Biophys Res Commun 332:392–397

Maeda H, Hosokawa M, Sashima T, Takahashi N, Kawada T, Miyashita K (2006) Fucoxanthin and its metabolite, fucoxanthinol, suppress adipocyte differentiation in 3T3-L1 cells. Int J Molec Med 18:147–152

Mann JE, Myers J (1968) On pigments, growth and photosynthesis of *Phaeodactylum tricornutum*. J Phycol 4:349–355

Martino AD, Bartual A, Willis A, Meichenin A, Villazán B, Maheswari U, Bowler C (2011) Physiological and molecular evidence that environmental changes elicit morphological interconversion in the model diatom *Phaeodactylum tricornutum*. Protist 162:462–481

McCleary BV, Draga A (2016) Measurement of beta-glucan in mushrooms and mycelial products. J AOAC Int 99:364–373

Meiser A, Schmid-Staiger U, Trösch W (2004) Optimization of eicosapentaenoic acid production by *Phaeodactylum tricornutum* in the flat panel airlift (FPA) reactor. J Appl Phycol 16:215–225

Michels MHA, Goot, Atze Jan van der, Vermuë MH, Wijffels RH (2016) Cultivation of shear stress sensitive and tolerant microalgal species in a tubular photobioreactor equipped with a centrifugal pump. J Appl Phycol 28:53–62

Mirón AS, García MC, Gómez AC, Camacho FG, Grima EM, Chisti Y (2003) Shear stress tolerance and biochemical characterization of *Phaeodactylum tricornutum* in quasi steady-state continuous culture in outdoor photobioreactors. Biochem Eng J 16287–297

Molina E, Martnez ME, Snchez S, Garca F, Contreras A (1991) Growth and biochemical composition with emphasis on the fatty acids of *Tetraselmis* sp. Appl Microbiol Biotechnol 36:21–25

Molina Grima E, Sánchez Pérez JA, García Camacho F, Fernández Sevilla JM, Acién Fernández FG, Urda Cardona J (1995) Biomass and icosapentaenoic acid productivities from an outdoor batch culture of *Phaeodactylum tricornutum* UTEX 640 in an airlift tubular photobioreactor. Appl Microbiol Biotechnol 42:658–663

Molina Grima E, Sánchez Pérez JA, García Sánchez JL, García Camacho F, López Alonso D (1992) EPA from *Isochrysis galbana*. Growth conditions and productivity. Process Biochem 27:299–305

Mus F, Toussaint J-P, Cooksey KE, Fields MW, Gerlach R, Peyton BM, Carlson RP (2013) Physiological and molecular analysis of carbon source supplementation and pH stress-induced lipid accumulation in the marine diatom *Phaeodactylum tricornutum*. Appl Microbiol Biotechnol 97:3625–3642

Myklestad SM (1989) Production, chemical structure, metabolism, and biological function of the (1→3)-linked, β3-D-glucans in diatoms. Biol Oceanogr 6:313–326

Nagarajan D, Lee D-J, Chen C-Y, Chang J-S (2020) Resource recovery from wastewaters using microalgae-based approaches: A circular bioeconomy perspective. Bioresour Technol 302:122817

Neumann U, Derwenskus F, Gille A, Louis S, Schmid-Staiger U, Briviba K, Bischoff SC (2018a) Bioavailability and safety of nutrients from the microalgae *Chlorella vulgaris*, *Nannochloropsis oceanica* and *Phaeodactylum tricornutum* in C57BL/6 mice. Nutrients 10:965

Neumann U, Louis S, Gille A, Derwenskus F, Schmid-Staiger U, Briviba K, Bischoff SC (2018b) Anti-inflammatory effects of *Phaeodactylum tricornutum* extracts on human blood mononuclear cells and murine macrophages. J Appl Phycol 30:2837–2846

Nunez M, Quigg A (2016) Changes in growth and composition of the marine microalgae *Phaeodactylum tricornutum* and *Nannochloropsis salina* in response to changing sodium bicarbonate concentrations. J Appl Phycol 28:2123–2138

Oscarsson J, Hurt-Camejo E (2017) Omega-3 fatty acids eicosapentaenoic acid and docosahexaenoic acid and their mechanisms of action on apolipoprotein B-containing lipoproteins in humans: A review. Lipids in Health and Disease 16:1–13

Peng J, Yuan J-P, Wu C-F, Wang J-H (2011) Fucoxanthin, a marine carotenoid present in brown seaweeds and diatoms: Metabolism and bioactivities relevant to human health. Mar Drugs 9:1806–1828

Petrushkina M, Gusev E, Sorokin B, Zotko N, Mamaeva A, Filimonova A, Kulikovskiy M, Maltsev Y, Yampolsky I, Guglya E, Vinokurov V, Namsaraev Z, Kuzmin D (2017) Fucoxanthin production by heterokont microalgae. Algal Res 24:387–393

Radwan S (1991) Sources of C20-polyunsaturated fatty acids for biotechnological use. Appl Microbiol Biotechnol 35:421–430

Rambjør GS, Wålen AI, Windsor SL, Harris WS (1996) Eicosapentaenoic acid is primarily responsible for hypotriglyceridemic effect of fish oil in humans. Lipids 31:45–49

Reis B, Gonçalves AT, Santos P, Sardinha M, Conceição LEC, Serradeiro R, Pérez-Sánchez J, Calduch-Giner J, Schmid-Staiger U, Frick K, Dias J, Costas B (2021) Immune status and hepatic antioxidant capacity of Gilthead Seabream *Sparus aurata* juveniles fed yeast and microalga derived β-glucans. Mar Drugs 19:653

Revellame E, Aguda R, Chistoserdov A, Fortela D, Hernandez R, Zappi M (2021) Microalgae cultivation for space exploration: Assessing the potential for a new generation of waste to human life-support system for long duration space travel and planetary human habitation. Algal Res 55:102258

Ritter JCS, Budge SM, Jovica F (2013) Quality analysis of commercial fish oil preparations. J Sci Food Agric 93:1935–1939

Rodolfi L, Biondi N, Guccione A, Bassi N, D'Ottavio M, Arganaraz G, Tredici MR (2017) Oil and eicosapentaenoic acid production by the diatom *Phaeodactylum tricornutum* cultivated outdoors in Green Wall Panel (GWP®) reactors. Biotechnol Bioeng 114:2204–2210

Ryan MT, Collins CB, O'Doherty JV, Sweeney T (2012) Effects of dietary beta-glucans supplementation on cytokine expression in porcine liver. J Animal Sci 90 Suppl 4:40–42

Sachindra NM, Sato E, Maeda H, Hosokawa M, Niwano Y, Kohno M, Miyashita K (2007) Radical scavenging and singlet oxygen quenching activity of marine carotenoid fucoxanthin and its metabolites. J Ag Food Chem 55:8516–8522

Stark KD, van Elswyk ME, Higgins MR, Weatherford CA, Salem N (2016) Global survey of the omega-3 fatty acids, docosahexaenoic acid and eicosapentaenoic acid in the blood stream of healthy adults. Progr Lipid Res 63:132–152

Stiefvatter L, Lehnert K, Frick K, Montoya-Arroyo A, Frank J, Vetter W, Schmid-Staiger U, Bischoff SC (2021) Oral bioavailability of omega-3 fatty acids and carotenoids from the microalgae *Phaeodactylum tricornutum* in healthy young adults. Mar Drugs 19

Størseth T, Kirkvold S, Skjermo J, Reitan KI (2006) A branched β-d-(1→3,1→6)-glucan from the marine diatom *Chaetoceros debilis* (Bacillariophyceae) characterized by NMR. Carbohydr Res 341:2108–2114

Stuyven E, Cox E, Vancaeneghem S, Arnouts S, Deprez P, Goddeeris BM (2009) Effect of β-glucans on an ETEC infection in piglets. Vet Immunol Immunopathol 128:60–66

Subitec GmbH (2022), Homepage. https://www.subitec.com/industrie/kultivierungsmodul/. Accessed 28 Oct 2022

Sullivan LM, Weinberg J, Keaney JF (2016) Common statistical pitfalls in basic science research. J Amer Heart Assoc 5

Sweeney T, Collins CB, Reilly P, Pierce KM, Ryan M, O'Doherty JV (2012) Effect of purified beta-glucans derived from *Laminaria digitata*, *Laminaria hyperborea* and *Saccharomyces cerevisiae* on piglet performance, selected bacterial populations, volatile fatty acids and pro-inflammatory cytokines in the gastrointestinal tract of pigs. Brit J Nutr 108:1226–1234

Tassoni D, Kaur G, Weisinger RS, Sinclair AJ (2008) The role of eicosanoids in the brain. Asia Pacific J Clin Nutr 17:220–228

The Culture Collection of Algae at the University of Göttingen (2022a), SAG-Catalogue: *P. tricornutum* 1090–1a. http://sagdb.uni-goettingen.de/detailedList.php?str_number=1090-1a. Accessed 28 Oct 2022

The Culture Collection of Algae at the University of Göttingen (2022b) SAG-Catalogue: *P. tricornutum* 1090–1b. http://sagdb.uni-goettingen.de/detailedList.php?str_number=1090-1b . Accessed 28 Oct 2022

The Culture Collection of Algae at the University of Göttingen (2022c) SAG-Catalogue: *P. tricornutum* 1090–6. http://sagdb.uni-goettingen.de/detailedList.php?str_number=1090-6. Accessed 28 Oct 2022.

Vonshak A (1990) Recent advances in microalgal biotechnology. Biotech Adv 8:709–727

Wang C, Lan CQ (2018) Effects of shear stress on microalgae – A review. Biotech Adv 36:986–1002

Xia S, Gao B, Li A, Xiong J, Ao Z, Zhang C (2014) Preliminary characterization, antioxidant properties and production of chrysolaminarin from marine diatom *Odontella aurita*. Mar Drugs 12:4883–4897

Yang R, Wei D, Xie J (2020) Diatoms as cell factories for high-value products: chrysolaminarin, eicosapentaenoic acid, and fucoxanthin. Crit Rev Biotech 40:993–1009